AIAA JOURNAL
Vol. 44, No. 11, November 2006

Bilevel Optimization and Postbuckling of Highly Strained Composite Stiffened Panels

W. Liu,* R. Butler,† A. R. Mileham,‡ and A. J. Green§
University of Bath, BA2 7AY Bath, United Kingdom

DOI: 10.2514/1.22206

The paper presents a bilevel strategy for the efficient optimum design of composite stiffened panels using VICONOPT, a fast-running optimization package based on linear eigenvalue buckling theory, and embracing practical composite design rules. Panel level optimization finds a minimum weight cross-sectional geometry based on a substitution of equivalent orthotropic plates for laminated plates. Optimization at the laminate level finds stacking sequences satisfying laminate design rules. VICONOPT models are validated with ABAQUS finite element models, and with experimental compressive testing of two blade-stiffened panels. The buckling and postbuckling behavior of the two panels, with initial buckling in the stiffeners and skin, respectively, is investigated in a high load and high strain range. The bilevel strategy is evaluated by the design of a relatively short *Z* stiffened panel which has been manufactured and tested, and also by design of a long wing cover panel with combined loads. The weight saving from the wing cover panel is 13% compared with an existing datum design. This demonstrated that the strategy is efficient, reliable, and extendable into the long panel range.

I. Introduction

SKIN-STIFFENER structures are extensively used in the aerospace field due to their structural efficiency in terms of stiffness/weight and strength/weight ratios. The application of such panels is primarily within fuselages and wing boxes, where the weight saving potential of composite materials compared with aluminum alloys is well known. However, the design of composite panels involves the optimization of a large number of mixed variables such as discrete values of ply thickness and continuously variable plate widths. Further complication arises when the expert knowledge required for laminate design is considered and when the panel is constrained by buckling under axial compression.

During the design of composite laminates against buckling, the full complexities of detailed modeling, analysis and optimization are compromised for the sake of efficiency [1]. The optimization of composite stiffened panels subjected to buckling constraints has been considered in many previous studies. Some of these have focused on the simplest modeling method of closed-form equations to investigate the structural efficiency of various stiffener shapes for minimum mass and costing. Kollár [2] reported a closed-form equation to determine the local buckling loads of composite structural members when the edges of the webs are rotationally restrained by the flanges. Using closed-form equations as buckling constraints for cost and weight minimization, Kassapoglou [3] found that "*J*" stiffeners give the lowest weight configurations whereas "*T*" (blade) stiffeners give the lowest cost configurations. However, the buckling analysis using closed-form solutions does not account for coupling between skin and stiffeners or for interaction between overall buckling and local buckling. These may affect the minimum weight and should be added for a more accurate analysis.

Presented as Paper 1826 at the 46th AIAA/ASME/ASCE/AHS/ASC Structures, Structural Dynamics & Materials Conference, Austin, Texas, 18–21 April 2005; received 3 January 2006; accepted for publication 7 April 2006.

*Research Assistant, Department of Mechanical Engineering; W.Liu@bath.ac.uk.

†Senior Lecturer, Head of Composites Research Unit, Department of Mechanical Engineering; R.Butler@bath.ac.uk.

‡Professor, Head of Department of Mechanical Engineering.

§Manufacturing Engineer, Department of Mechanical Engineering.

Methods that account for interactive effects have been developed using finite strip elements, which divide panel segments into strips and represent the displacement in the strips using polynomial and trigonometric functions. Butler and Williams [4] performed design optimization of stiffened panels using the finite strip method within the program VICONOPT [5]. Lillico et al. [6] applied VICONOPT to aluminum alloy stiffened panels, considering constraints on the buckling load and also on the postbuckling maximum strength. The comparisons with the finite element (FE) package ABAQUS showed good agreement.

Use of FE Analysis (FEA) for optimization of stiffened panels, which frequently requires remeshing, is computationally expensive. Because of the discreteness of ply thickness, integer programming has been applied for the optimization of composite panels. Nagendra et al. [7] designed such panels based on an improved genetic algorithm (GA), combined with the PASCO [8] program to evaluate both buckling load and strain constraints. More recently, Bisagni and Lanzi [9] presented a postbuckling composite design method using a neural network to reduce the cost and complexity of an FE model. They applied the method to design of woven composites with an *L* shaped stiffener on both flat and curved skins. The preliminary design stage requires consideration of structural efficiency of stiffened panels with different shaped stiffeners. Also, when using unidirectional tape for fabrication of thick stiffened composite panels, the requirement of stacking sequences becomes more complicated than for woven composites. As a result, the cost of computation, including genetic searching, fitness training, and FE calculation, may increase significantly.

Nagendra et al. [10] also considered the use of PASCO continuous optimization to design a blade-stiffened composite panel with a hole. To achieve the integer laminate thickness, rounding-off was used for every layer group within the skin laminate and stiffener laminate. The disadvantage of this approach is that it does not satisfy laminate design rules, which will be described in the next section. Such designs are also likely to be heavy compared with the optimum designs produced using a GA technique [7]. Furthermore, when designing a composite aircraft wing, GA optimization has difficulty satisfying continuity constraints between panels because the optimum designs of adjacent panels are likely to have completely different stacking sequences.

The objective of this paper is not only to design stiffened composite panels efficiently by combining discrete and continuous optimization, but also to take into account design and manufacturing

constraints. The bilevel strategy proposed includes continuous panel level optimization of the cross-sectional panel dimensions and discrete laminate level design of the stacking sequences. The panel level optimization uses VICONOPT continuous optimization and the laminate level design only rounds-off the whole laminate thickness once. This reduces the weight penalty compared with rounding off every layer group. The paper consists of three sections: namely the validation of the VICONOPT and FE results by experimental compression testing of two blade-stiffened panels that have been specifically designed with initial buckling in the stiffeners and skin, respectively. The bilevel optimum design strategy for composite stiffened panels is then described. This is followed by the optimum design example of a Z stiffened panel including a comparison of experimental testing data and ABAQUS analysis for this panel. Finally, long wing cover panel optimum designs obtained from the strategy are reported with weight saving comparison with an existing datum design.

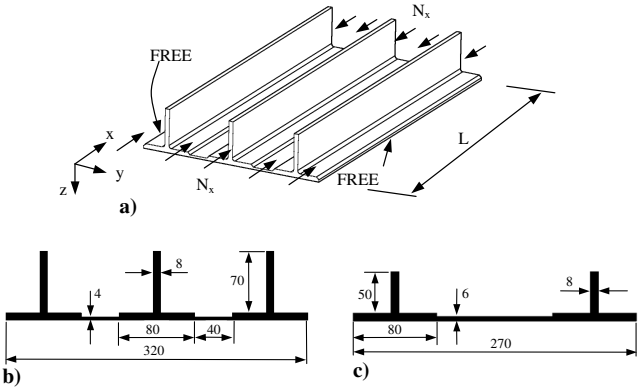

Fig. 1 Panel geometry and boundary conditions: a) Isometric view. Cross sections of b) 3-blade-stiffened panel, and c) 2-blade-stiffened panel. All dimensions are in mm.

II. Blade-Stiffened Panels: Analysis and Experimental Testing

A. Example Panels

The stiffened panels, made of carbon fiber reinforced plastic (CFRP) unidirectional UTS/977-2 prepreg, were subject to axial compressive load, and had free longitudinal edges and clamped transverse edges. The material ply thickness was 0.25 mm, and the following properties were assumed: $E_{11} = 117$ GPa, $E_{22} = 17$ GPa, $G_{12} = 4.6$ GPa, and $\nu_{12} = 0.3$, and density and $\rho = 1584$ kg/m^3. The final configurations were designed using VICONOPT, combined with expert knowledge, that is, best practice and lessons learned from previous structural design, analysis and testing of composites. The design target was a high strain and high load range, that is, the strain was around 4000 microstrain, and the compressive design load per unit width was approximately 4 kN/mm. The four orientations 45, −45, 0 and 90 deg of plies were used, where 0 deg is parallel to the direction of load.

During laminate design, various rules [11] arising from expert knowledge were employed. For example,

1) The 10% rule design was applied to prevent direct loading of the matrix in any direction. As a result, there were at least 10% of 90 deg plies within skin laminates and stiffener laminates.

2) At least 40% of ±45 deg plies were used in the skin (and 30% in the stiffeners) to maximize bearing strength for assembly by mechanically fastened joints.

3) Grouping of more than 3 plies of the same orientation together was avoided to minimize edge splitting and maintain a homogeneous stacking sequence.

4) The outer plies of the skin and stiffener laminate were ±45 deg plies to take damage tolerance aspects under compressive loading into consideration.

Two blade-stiffened panels were designed according to the design target and rules. The loading, boundary conditions and geometry of the two panels are illustrated in Fig. 1. The loaded edges are fully restrained in rotation and restrained in displacement in y and z. The longitudinal edges are free. For the 3-blade-stiffened panel, the skin has a stacking sequence of $[45/-45/0_2/90/0_2/45/-45/0_2/90/0_2/-45/45]$, and the stiffener blade $[45/0/-45/0_3/90/0_2/90/0_3/-45/0/45]_S$. For the 2-blade-stiffened panel, the skin has a stacking sequence of $[45/-45/0_2/90/0/45/-45/0_2/90/0]_S$, and the stiffener blade has the same stacking sequence as that of the 3-blade-stiffened panel. The stiffener flanges for both panels have half the stacking sequence of the stiffener blades with an additional two plies of ±45 on the bottom to seal the wedge of filler inside the stiffener base. Both panels satisfied the laminate design rules with around 50% of 0 deg material in skin and 60% of 0 deg material in the stiffeners. The length of the 3-blade-stiffened panel and the 2-blade-stiffened panel was $L = 500$ and $L = 550$ mm, respectively. The two blade-stiffened panels were not optimum because different initial buckling modes were to be investigated, that is, stiffener buckling and skin buckling.

B. VICONOPT Background

VICONOPT [5] is a computer program covering calculation of critical buckling load factors, or undamped natural frequencies and mode shapes of isotropic or anisotropic prismatic plate assemblies, each of which can carry any combination of uniformly distributed and longitudinally invariant in-plane stresses. It can be utilized as an analysis or optimum design program. The eigenvalue analysis uses a transcendental stiffness matrix derived from exact solution of the governing differential equations of the constituent members, which are assumed to undergo a deformation that varies sinusoidally to infinity in the longitudinal direction. This, accounting for the continuity over several bays of typical aerospace structures, may influence the agreement of critical buckling loads between VICONOPT and single bay results [12] of FEA and experimental test panels. The minimum weight optimization of the panel is performed subject to buckling, material strength and geometric constraints. Any set of plate widths, ply thickness and stiffener spacing can be selected as independent design variables, whereas the other dimensions can be held fixed or can be linked to the design variables. The continuous optimum solution is obtained by using a gradient-based search with a thickness factoring procedure. A nearby discrete solution that satisfies the constraints can then be chosen as the optimum design.

C. FEA Modeling

The general-purpose code ABAQUS [13] is employed to create FE models of the panels using the four-node general element S4R with 6 degrees of freedom at each node and three integration points along the thickness of each ply. This element can account for transverse shear deformation. With the skin thickness of 4 or 6 mm and the stiffener thickness of 8 mm, the transverse shear deformation of the panel is more influential than that of metal panels of the same geometry. The dimension of the element was set to 5×5 mm. Both linear eigenvalue analyses and nonlinear static analyses, using a modified Riks method, were performed to study buckling and postbuckling behavior of the panels.

To model the offsets between the flange and the skin; and between the web and the skin, the skin and stiffeners was meshed as separate components, and then joined together using the multipoint control technique of ABAQUS. The bottom plane of the blade stiffener is located as the reference plane by adding negligibly low stiffness material on the surfaces of the skin and the flange. In this way, the skin nodes and the flange nodes can be moved to the same reference plane, and then constrained with identical translations and rotations. This approach ensures continuity of the skin. In addition, ABAQUS nonlinear analysis for the two panels were calculated with a full cos-wave imperfection over the length of the panel of amplitude 0.5 mm causing increased compression in the stiffener at the panel center. The reason for this was that the two manufactured panels had global imperfection due to spring-back following cure of the composite parts.

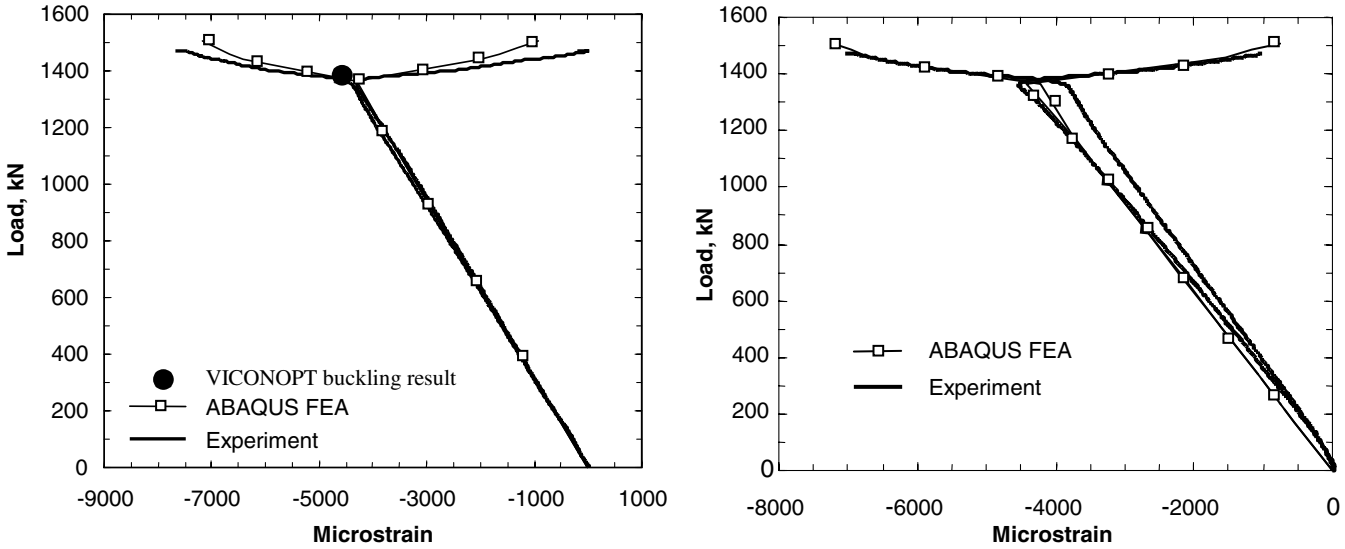

Fig. 2 Strain in back-to-back gauges on the two side stiffeners at quarter length distance from 3-blade-stiffened panel end.

D. Experimental Testing and Results

The two blade-stiffened panels were manufactured, using an autoclave with controlled pressure and temperature in the University of Bath. An aluminum mold was designed and machined to fabricate the blade stiffeners. The stiffeners and skin were laminated by hand lay-up and then bagged by a standard composite bagging system with a bleeder. They were cured separately in the autoclave and then bonded together using FM-300 film adhesive. Ultrasonic *C*-scan was employed to check for defects in the panel at various stages during this manufacturing process.

The two blade-stiffened panels were strain gauged to monitor the onset and advance of buckling, which was found to be more accurate than load versus end-shortening plots. The upper end and the lower end were potted into a 25 mm thick block of epoxy resin to achieve the clamped end fixture. The skin side opposite the stiffeners was painted white for the application of a Moiré shadow to observe buckling patterns of the panel as they developed during the compression tests. The grating frequency was 2 lines/mm. White lines were drawn on the tips of stiffeners to indicate the buckling shape from the stiffener side. Two high resolution digital cameras were set at each face of the test panel to record the Moiré fringe and stiffener deformation.

Tests were performed using a Dartec 2000 kN testing machine under displacement control. The stroke rate was 0.01 mm/second before buckling and 0.005 mm/s after buckling. To ensure uniform loading, the panels were pretested to 500 kN and the crosshead platen adjusted until all strain gauges displayed approximately the same reading. Because the prediction from VICONOPT and ABAQUS indicate that the critical buckling loads occur above 1000 kN, initial buckling loading was performed to 1200 kN for the 3-blade-stiffened panel, and to 1000 kN for the 2-blade-stiffened panel, respectively. After the initial buckling testing, the panels were loaded to failure.

The 3-blade-stiffened panel was designed to buckle in the stiffeners initially. Figure 2 presents the experimental results obtained with the strain gauges located on the two side stiffeners at a quarter of the length of the panel from the upper loading edge. The strain gauges were placed back-to-back near the free edge of the stiffener. It can be seen that buckling occurs when the loading reaches 1378 kN, and a strain of 4400 microstrain. For comparison, the FEA results are also presented in the figure, showing good agreement. The results from VICONOPT, ABAQUS and experimental testing are summarized in Table 1. In all cases, the three stiffeners buckled into between two and three half-wavelengths over the panel length during testing.

It was noted that, according to the Moiré pattern, there was no obvious out-of-plane deformation on the skin. This was coincident with FEA results. Both show that the maximum out-of-plane deformation at the antinodal line was less than 0.25 mm. It is also shown that the actual imperfection of the panel did not significantly affect the advance of buckling and postbuckling in the stiffener.

The strain data shows that the panel has little postbuckling capacity after such high initial stiffener buckling strain. The panel buckled at 1378 kN and then failed at 1472 kN, which is about 7% above the initial buckling load. There was no evidence of overall buckling until the panel failed. It seems that the buckling deformation tended to pull the stiffeners from the skin because the failed panel indicates separation of stiffeners from skin.

The 2-blade-stiffened panel was designed for initial buckling to occur in the skin. In comparison with the previous panel, this panel has more imperfection sensitivity due to its lower overall bending rigidity, which causes a lower Euler buckling load. This is evident in Table 1, which shows that with the same shape and amplitude of global imperfection, the nonlinear buckling load of the 3-blade panel is 2% less than the linear result, whereas for the 2-blade panel, the difference is 5%. This was also observed during the pretesting, where the 2-blade panel presented greater difficulty in achieving uniform strain than the 3-blade panel due to the effect of imperfection. The Moiré pattern shown in Fig. 3 demonstrates obvious out-of-plane deformation of the skin in the form of between two and three half-wavelengths over the panel length, which is coincident with the

Table 1 Summary of initial buckling results for blade-stiffened panels

Panels	Results	VICONOPT[a]	ABAQUS		Experiment
			Linear	Nonlinear[b]	
3-blade	Initial buckling load (kN)	1397	1396	1362	1378
	Initial buckling strain (10^{-6})	4482	——	4330	4400
2-blade	Initial buckling load (kN)	1259	1205	1150	1160
	Initial buckling strain (10^{-6})	5331	——	4649	4528

[a]No imperfection for VICONOPT results.
[b]ABAQUS nonlinear results calculated with a full cos-wave imperfection over the length of the panel of amplitude 0.5 mm causing increased compression in the stiffener at the panel center.

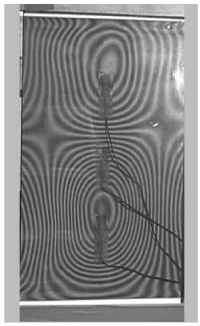

Fig. 3 Moiré pattern of post-buckled 2-blade-stiffened panel.

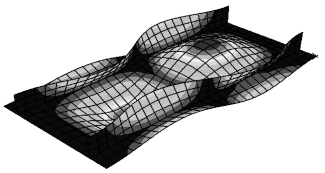

Fig. 4 ABAQUS prediction of buckling mode for 2-blade-stiffened panel.

VICONOPT and ABAQUS analysis results, see Fig. 4. The initial buckling loads shown in Table 1 are also in good agreement. However, Fig. 5b indicates that there are some differences between the postbuckling strains of the experimental test and those predicted by FEA. This is probably due to differences in the boundary conditions of the FEA model, and the experimental test. The boundary conditions assumed in the FEA model are rotational restraints at both loaded edges of the panel, whereas for the test, the upper loading platen is universally jointed, allowing free rotation after buckling occurs. The influence of these differences on postbuckling behavior has been considered for metallic panels in [6,12].

III. Bilevel Optimum Design Strategy

The goal of the optimization is to find the stacking sequence and cross-sectional geometry of minimum weight panels that will not buckle or fail due to excessive strains for a particular set of design loads and boundary conditions. The optimum design of the Z stiffened panel presented in Sec. IV will observe the laminate design rules shown above and will also use VICONOPT, the design objective of which is to minimize mass. For standard VICONOPT design, stacking sequences are always selected before optimization. However, this approach will invariably produce an optimum design that does not satisfy the above laminate design rules. For example, an initial stacking sequence chosen as $[45/-45/90/0]_S$ might produce the optimum laminate $[45/-45/90/0_5]_S$, which has 10 plies of 0 deg orientation grouped in the middle of the laminate, and does not therefore satisfy the ply grouping rule.

A new bilevel VICONOPT strategy for practical optimum design of composite stiffened panels is proposed and illustrated in Fig. 6.

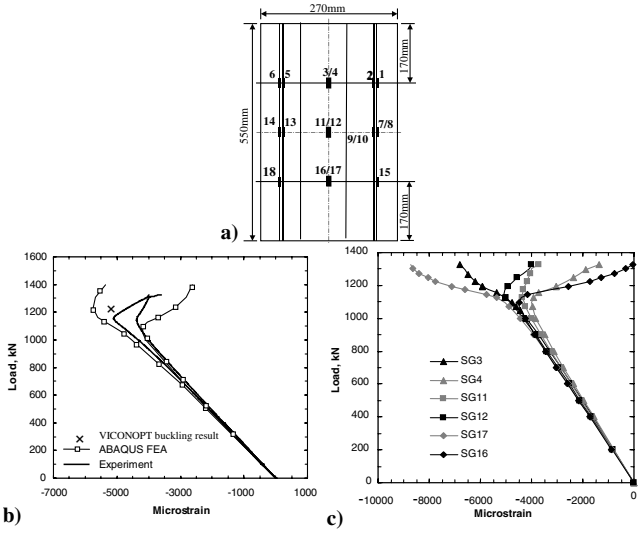

Fig. 5 Strain on the 2-blade-stiffened panel, a) strain gauge positions, b) strain from SG11 and SG12, and c) strain from experiment in the center of the skin.

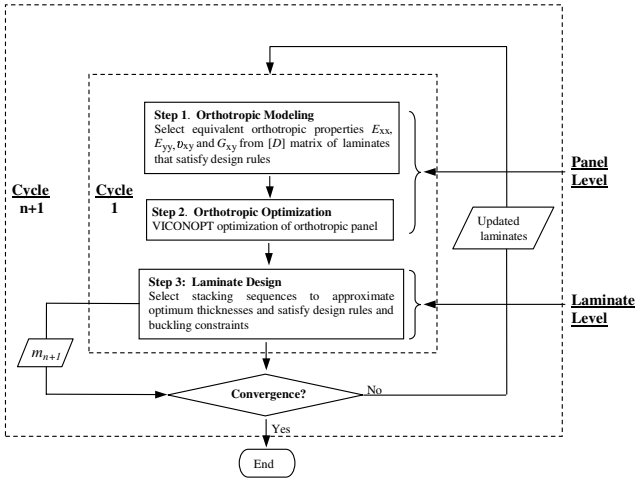

Fig. 6 Bilevel optimization strategy.

The panel level, which includes Steps 1 and 2, treats laminates as orthotropic plates of continuous thickness to find the optimum panel cross section. Initially, the material properties of these orthotropic plates are selected from existing stacking sequences that satisfy the laminate design rules. Note that the orthotropic properties arising from the laminate $[A]$ matrix do not vary with thickness whereas Fig. 7 shows that this is not the case when the $[D]$ matrix is used. Hence the properties arising from $[D]$ are used because buckling is primarily governed by the $[D]$ matrix of each laminate. The properties of Step 1 are obtained from the equations given in the Appendix.

Table 2 presents the stacking sequences of typical skin laminates. Their $[D]$ matrices were used to calculate the equivalent orthotropic material properties in Fig. 7. The percentage of 0, ± 45, and 90 deg plies were different between the skin and the stiffener. The skin has about 50% of 0 deg, 40% of ± 45 deg, and 10% of 90 deg plies, whereas the stiffeners have 60% of 0 deg, 30% of ± 45 deg, and 10% of 90 deg plies. For brevity, only the data for the skin is presented here because the stiffener plot follows similar trends. The average of the equivalent orthotropic material properties of the 10 mm skin and the 10 mm stiffener were used at the beginning of the orthotropic optimization procedure.

VICONOPT minimum mass optimization is performed during step 2 using the equivalent orthotropic material properties obtained from step 1. Any set of plate widths and thicknesses can be selected as design variables. Other plate widths and offsets may be held fixed or linked to the design variables. Note that the orthotropic plate thicknesses are continuous variables and can readily be optimized using the gradient-based optimizer within VICONOPT.

Once the optimum orthotropic panel design with continuous thickness values has been found, the laminate level of optimization is started. The aim of this level (step 3 of Fig. 6) is to substitute the

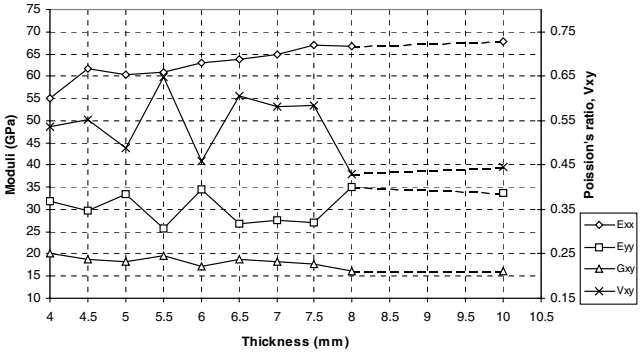

Fig. 7 Equivalent orthotropic material properties from $[D]$ matrix for laminates in Table 2.

Table 2 Stacking sequences for typical skin laminates

Thickness (mm)	Stacking sequence	Percentage of 0/ ± 45/90 material
4.0	$[\pm 45/0_2/90/0_2/\pm 45/0_2/90/0_2/\mp 45]$	50.0%/37.5%/12.5%
4.5	$[\pm 45/0_3/90/0_2/\pm 45/0_2/90/0_3/\mp 45]$	55.6%/33.3%/11.1%
5.0	$[\pm 45/0_2/90/0_2/\pm 45/0]_S$	50.0%/40.0%/10.0%
5.5	$[\pm 45/0_3/90/0_2/\pm 45/0]_S$	54.5%/36.4%/9.1%
6.0	$[\pm 45/0_2/90/0_2/\pm 45/0/90/0]_S$	50.0%/33.3%/16.7%
6.5	$[\pm 45/0_3/\pm 45/0_2/90/0/90/0]_S$	53.8%/30.8%/15.4%
7.0	$[\pm 45/0_3/\pm 45/0_2/90/0/90/0/45/-45/0/90/0/90/0_2/\mp 45/0_3/\mp 45]$	50.0%/35.7%/14.3%
7.5	$[\pm 45/0_3/\pm 45/0_3/90/0/90/0/45/-45/0/90/0/90/0_3/\mp 45/0_3/\mp 45]$	53.3%/33.3%/13.4%
8.0	$[\pm 45/0_2/90/0_2/\pm 45/0_2/90/0/\pm 45/0]_S$	50.0%/37.5%/12.5%
10	$[\pm 45/0_2/90/0_2/\pm 45/0_2/\pm 45/0_2/90/0/\pm 45/0]_S$	50.0%/40.0%/10.0%

Table 3 VICONOPT sizing cycles for step 2 of cycle 1

VICONOPT cycle	B_1 (mm)	B_2 (mm)	B_4 (mm)	T_1 (mm)	T_2 (mm)	Mass (kg)
Initial	50.0	50.0	45.0	5.00	4.00	2.82
1	37.3	37.3	33.5	3.92	3.94	2.14
2	42.0	32.4	29.4	4.08	3.57	2.03
3	42.1	32.5	29.3	4.08	3.56	2.03
4	42.1	32.5	29.3	4.08	3.56	2.03

orthotropic plates with laminated plates with minimum mass penalty, and also satisfying the buckling constraints and the laminate design rules. The continuous variables therefore need to be rounded down or up due to the discrete nature of laminate thickness. First, every design variable is rounded down to its nearest discrete value to produce the laminate design. The stacking sequences of the laminate are selected based on the design rules. (Manufacturing constraints could also be applied at this stage. For example, such constraints could maintain continuity of plies for adjacent panels.) If the design can carry the design load without buckling, which is checked using VICONOPT analysis, the laminate design is feasible. Otherwise, the thicknesses are increased ply by ply until a check with VICONOPT analysis confirms that the laminate design satisfies all the constraints. In particular, it is seen in the next section that there are only two discrete design variables involved in this method for composite stiffened panels, that is, skin thickness and the stiffener thickness. Hence, the method has fewer variables than other methods, which treat every ply as design variable [14]. This reduces computational time significantly, and so giving a practical advantage to the optimization of composite skin-stiffener structures.

The mass m_1 of the feasible laminate design is calculated at the end of the first cycle. The second cycle then starts with the updated equivalent orthotropic material properties obtained from the feasible design of the first cycle to check for convergence. The reason for this is to ensure that the design is optimum for this design region, that is, within this region of plate thicknesses. The orthotropic material properties for the second cycle are an average of those calculated from the skin and stiffener laminates of the feasible design of the first cycle. Note that the value of maximum allowable strain may require modification to compensate for the updated value of E_{xx}. Note also that the orthotropic material properties obtained from the $[D]$ matrix converge to those from the $[A]$ matrix when the laminates are around 40 plies thick. This means that the method will become more robust when laminates contain a large number of plies.

After the second orthotropic optimum design is obtained in step 2, the sequential rounding in step 3 finds the laminate design satisfying the design rules, and buckling and strain constraints. The mass m_2 of the design is calculated and compared with m_1 of the first cycle. If $m_1 \leq m_2$, the feasible design of the first cycle proves to be optimum. If $m_1 > m_2$, the laminate design from the second cycle can be selected as an optimum design or cycling may continue by averaging the two orthotropic material properties and finding the next possible lighter design. Typically, it takes VICONOPT about 2 minutes to complete an optimization step, and even less time to analyze a laminate design. Hence several cycles can be finished in a short time with the added advantage of accurate prediction of buckling loads for the optimum design.

IV. Application Examples of Bilevel Optimization Strategy

In this section, two design examples are presented to evaluate the bilevel optimization strategy. First, the optimum design procedure of the Z stiffened panel is presented step by step, including initial design requirements, and panel level, and laminate level optimization. The VICONOPT predicted buckling load of the panel is compared with FEA analysis results and experimental data. The postbuckling behavior is investigated by experimental testing and ABAQUS nonlinear analysis with various imperfections. The bilevel optimization strategy is then extended to long wing cover panels designed to carry combined loading.

A. *Z*-Stiffened Panel

1. *Optimum Design*

The bilevel optimization strategy was evaluated by the design of a Z stiffened panel with free longitudinal edges and clamped transverse edges. The material described in Sec. II was again used. The panel was designed to carry a compressive load of 2.8 kN/mm without buckling and with a maximum allowable midsurface strain of 5000 microstrain in any plates. The length of the panel was $L = 550$ mm.

The optimization strategy started with an average of the equivalent orthotropic material properties, obtained from 10 mm thick skin and stiffener, see Fig. 7 for the skin, which is $E_{xx} = 68$ GPa, $E_{yy} = 34$ GPa, $G_{xy} = 16$ GPa, and $\nu_{xy} = 0.44$. The equivalent orthotropic material properties for the stiffener were $E_{xx} = 75$ GPa, $E_{yy} = 33$ GPa, $G_{xy} = 14$ GPa, and $\nu_{xy} = 0.41$. Therefore, the average of these values was used as the input material properties for step 1 of cycle 1 and then for the optimization of step 2 of cycle 1.

All the design variables used in step 2 are illustrated in Fig. 8. The width of the panel was fixed to 300 mm, and the width of the flange B_1 was constrained to be greater than 40 mm. Hence B_1, B_2, B_4, T_1, and T_2 were independent variables, whereas B_3 was dependent and linked with the width of the panel and B_1. The optimizer could

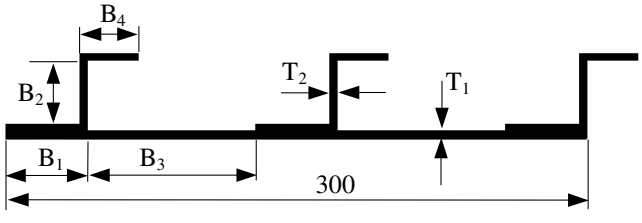

Fig. 8 Cross section of *Z* stiffened panel with design variables.

Table 4 Optimization results for *Z* stiffened panel

	Cycle 1			Cycle 2		
	Step 1[a] Initial design	Step 2[a] Orthotropic optimization	Step 3[b] Laminate design	Step 1[a] Initial design	Step 2[a] Orthotropic optimization	Step 3[b] Laminate design
B_1 (mm)	50	42.1	42	42	42.9	43
B_2 (mm)	50	32.5	33	33	33.7	34
B_3 (mm)	75	86.9	87	87	85.7	86
B_4 (mm)	45	29.3	30	30	30.6	31
T_1 (mm)	5	4.08	$[45/-45/0_2/90/0_2/45/-45/0_2/90/0_2/-45/45]$	4	3.82	4
T_2 (mm)	4	3.56	$[45/-45/0_3/90/0]_S$	3.5	3.74	3.5
E_{xx} (GPa)	72.0	72.0	——	55.0	55.0	——
E_{yy} (GPa)	33.5	33.5	——	31.9	31.9	——
G_{xy} (GPa)	15.0	15.0	——	19.9	19.9	——
ν_{xy}	0.42	0.42	——	0.53	0.53	——
Mass (kg)	2.82	2.03	2.00	2.00	2.05	2.04
N_{cr} (kN/mm)	3.50	2.84	2.88	3.01	2.90	2.86

[a]The critical buckling loads N_{cr} for steps 1 and 2 assumed orthotropic properties.
[b]The step 3 laminate design of cycle 1 is taken as the final optimum.

select any set of design points within the feasible domain that satisfy the buckling constraint and the strain constraint. The VICONOPT sizing cycles are reported in Table 3. The final optimization results are also summarized in Table 4 with the optimum laminate design of the panel (step 3 of cycle 1).

When VICONOPT analysis of the optimum design was performed, the initial buckling load N_{cr} was calculated as 2.88 kN/mm and the buckling strain was 5053 microstrain, indicating that the design was feasible in terms of strength and stiffness requirements. To ensure the design was optimum, the updated orthotropic material properties were used in a second cycle of optimization. The updated orthotropic optimum result gave 2% increase in mass, see Table 4 and so the laminate panel design of the first cycle was taken as optimum.

Table 4 also presents the N_{cr} for each design after each step. It is noted that when the very different orthotropic material properties were used for the two panels of similar geometry (step 2 of the first cycle compared with step 1 of the second cycle), there is only about 6% difference in the N_{cr} of the two panels, although the second cycle E_{xx} of 55 GPa is 24% lower than the 72 GPa used in the first cycle. It is assumed that the reason for this is the associated increase in G_{xy} and ν_{xy} values for the design of the second cycle, which results in larger stiffness terms D_{12} and D_{66}, producing similar values of N_{cr} for the two designs. The laminated design N_{cr} of 2.88 kN/mm for step 3 of the first cycle is 4% lower than the orthotropic design N_{cr} of 3.01 kN/mm for step 1 of the second cycle. This difference is attributed to the nonvanishing bending-twisting coupled stiffness terms D_{16} and D_{26} in the laminate design. The difference, which is due to the relative position of +45 and −45 deg materials, will reduce for laminates containing more plies.

2. *Postbuckling Analysis*

ABAQUS FEA was applied to the *Z* stiffened panel to verify the VICONOPT design results. The initial buckling load N_{cr} calculated by linear FEA was 2.85 kN/mm. This was close to the VICONOPT prediction result of 2.88 kN/mm. Figure 9 shows the initial buckling modes of the panel predicted by VICONOPT and ABAQUS. To illustrate the computational advantage of the strip model, VICONOPT required 5 elements for the skin whereas ABAQUS required over 7,000 elements for the skin. Both indicate that the panel buckles into between four and five half-wavelengths over the panel length.

To verify the optimum design of *Z* stiffened panel, the panel was manufactured for experimental compression testing, see Fig. 10. During manufacture, it was found that the *Z* stiffener was more difficult to fabricate than the blade stiffener due to the more complicated tooling with double curvature. It was noted that, due to practical manufacturing constraints, the final specimen has a 5 mm inner radii between the web and flange. However, the optimization model has a 90 deg corner at this junction, referring to Fig. 8. After modeling the radii, which increases the exposed width of the skin, it was found that the updated critical buckling loads are, respectively, 13% and 17% lower than the previous straight plate models of VICONOPT and ABAQUS. To correspond to the experimental specimen, the following VICONOPT and nonlinear FE results use the updated model with the radii.

During the nonlinear analysis, it was found that the Riks arc length analysis of the perfect panel model was not able to pass the first bifurcation point due to severe discontinuity around that point. The end shortening versus load for the perfect model indicated that the critical buckling load was approximately 750 kN (2.5 kN/mm), although the initial buckling mode shape was not coincident with the linear eigenvalue analysis result. It was found that in order to perform nonlinear analysis in the postbuckling field with the correct initial buckling mode shape, a small initial imperfection in the shape of the initial mode was required. The lowest amplitude of this mode was found to be 0.01 mm. However, as is well known, imperfections cause reduction of the initial buckling load. For this *Z* stiffened panel, the 0.01 mm and 0.1 mm imperfection caused 6 and 10% reduction of the initial buckling load, respectively. Therefore, it seems that the optimum design of the *Z* stiffened panel has more bifurcation paths

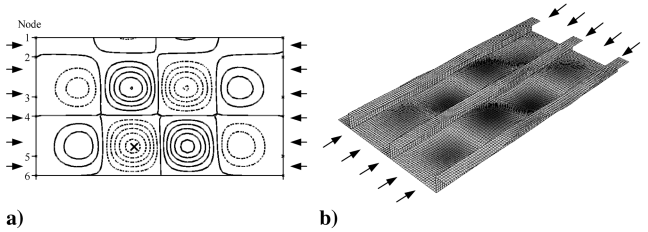

a) b)

Fig. 9 Initial buckling mode of *Z* stiffened panel, a) VICONOPT contour plot of the skin; b) ABAQUS isometric plot. Cross in a) shows the location of skin strain gauges.

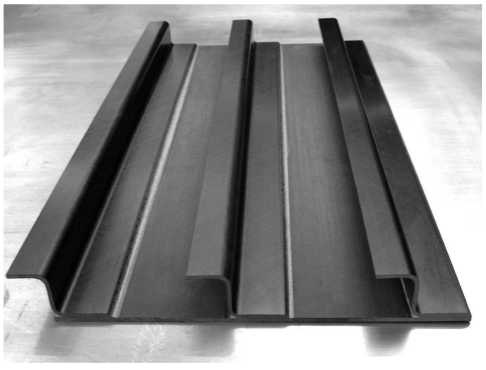

Fig. 10 *Z* stiffened panel test specimen.

around the first bifurcation point than the two blade-stiffened panels, for which the analysis easily picked up the first bifurcation path without needing to add the scaled initial imperfection to the nonlinear postbuckling analysis. This may be due to the optimization and due to the increased number of local buckling modes that occur in the *Z* stiffened panel.

Although the analysis could follow the equilibrium path beyond the first bifurcation point, the Riks arc length method could not converge around the second bifurcation point. Because the experimental panel failed locally before reaching the second bifurcation point, the Riks arc length method was adequate. If analysis beyond a stable second bifurcation was required, the Newton method may have been more suitable.

3. *Experimental Test*

The panel was end-potted, and loaded in compression to failure with controlled displacement of 0.01 mm/second before buckling and 0.005 mm/second after buckling. Fifteen strain gauges were attached to the panel to record initiation of critical buckling and the post-buckled deformation. A Moiré shadow technique was applied to identify the buckling mode, which indicates that the panel buckled into four half-wavelengths over the panel length coincident with the VICONOPT and FEA linear analysis result of Fig. 9.

The strain reading from two back-to-back gauges versus the compressive load is presented in Fig. 11, where the location of the strain gauges is shown in Fig. 9 a). The strain data shows that the panel buckled at 770 kN and then failed at 950 kN, which is about 24% above the initial buckling load. Compared with the blade-stiffened panels, the *Z* stiffened panel has an increased postbuckling capacity.

The strain data were also compared with ABAQUS nonlinear results, see Fig. 11. Although the buckling and postbuckling behavior follows the same bifurcation path, the buckling load from testing is 6% higher than the nonlinear FEA result with a 0.01 mm imperfection. This difference is attributed to the following two factors. First, the added imperfection will reduce initial buckling loads. Second, it is worth pointing out that the material properties of Sec. II were used in all VICONOPT and ABAQUS models. These properties are obtained from the *B*-basis statistical procedure, used to derive material properties and allowables. The property value indicated is the value above which at least 90% of the population of values is expected to fall with a confidence of 95%. Compared with mean values, *B*-basis values are conservative.

B. Long Wing Cover Panel

The bilevel optimization strategy was presented and performed to design a *Z* stiffened panel in the previous section. In particular the panel was manufactured and then tested to failure to validate the optimal design. Because of constraints of manufacture and experimental testing, the length of the panel was limited to 550 mm and the boundary condition was clamped. However, actual aircraft wing panels are longer than this and are often assumed to be simply supported by ribs. Accordingly, the present work is extended to long wing cover panels designed to carry combined loading

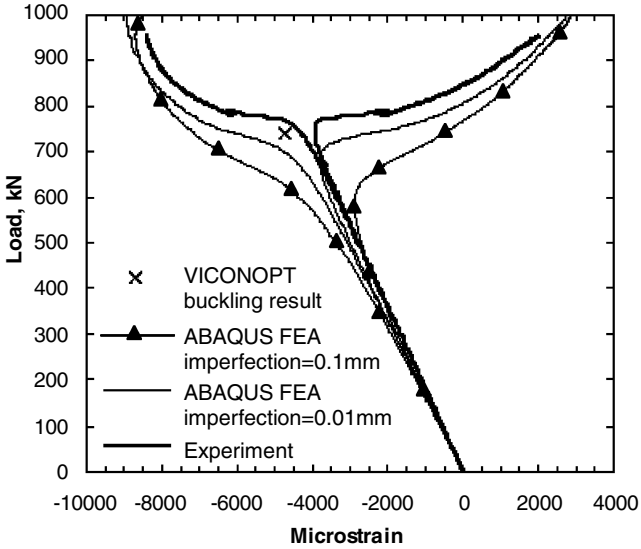

Fig. 11 Strain in back-to-back gauges on the skin of *Z* stiffened panel.

(compression, shear and pressure) using the bilevel optimization strategy. In this section, the long panel design requirements are firstly defined. This is followed by presentation of the optimal design.

1. *Problem Definition*

The long wing cover panel is designed for the wing of a typical transport aircraft with four engines. The panel is located between two engines in the upper section of a 770 mm rib bay, that is, panel length of 770 mm. The panel is therefore subject to a small pressure load of 0.109 N/mm^2, owing to fuel that fills the wing boxes within that area. The panel is also designed to carry a compression load N_x of 1.91 kN/mm, and a shear load N_{xy} of 0.10 kN/mm applied to the skin only. The full width panel consists of 15 stiffeners. Based on the blade stiffener concept, the mass per unit planform area of an existing datum design of the panel is 14.4 kg/m^2, see Table 5 and Fig. 12a. Accordingly, the objective of this optimization is to find a stiffened panel that is lighter than the existing datum design and can carry the combined loads without buckling and with maximum strains below 3600 microstrain. The panel is made of CFRP IM tape with material properties: $E_{11} = 131$ GPa; $E_{22} = 7.1$ GPa, $G_{12} = 3.5$ GPa; $\nu_{12} = 0.3$, and $\rho = 1584$ kg/m^3. The panel is assumed to be simply supported at ribs for buckling analysis, and clamped at ribs for out-of-plane bending due to pressure; causing increased compression in the stiffeners at panel midlength and increased compression in the skin at panel ends.

2. *Optimum Design Results*

The VIPASA-type infinite width analysis within VICONOPT and the bilevel optimization strategy were applied to obtain an optimum design. The design laminate target for the percentages of $0/\pm 45/90$ material was 60/30/10 respectively. Target maximum strain was

Table 5 Design of long wing cover panel

Design		Configuration	$0/\pm 45/90$ percentage
Existing datum design		Fig. 12a	
$N_{cr}/N_x = 1.21$			
$\varepsilon_{max} = 3590(\times 10^{-6})$	Skin[a]	$[+45/-45/0/0/90/0/-45/0/+45/+45/0]_S$	44%/44%/12%
	Web	$[+45/0/0/-45/0/0/90/0/45/0/0/-45/0/90/0/0/45/0/-45/0/0/45/\frac{0}{2}]_S$	60%/30%/10%
	Flange	$[+45/0/0/-45/0/0/90/0]_S$	63%/25%/13%
New optimum design		Fig. 12b	
$N_{cr}/N_x = 1.06$			
$\varepsilon_{max} = 3680(\times 10^{-6})$	Skin	$[+45/-45/0/0/0/90/0/0/+45/-45/0/0/90/0/0/0/+45/-45]_T$	56%/33%/11%
	Web	$[+45/-45/0/0/0/+45/-45/0/0/0/0/90/0/0/0/\frac{90}{2}]_S$	62%/28%/10%
	Flange	$[45/-45/0/0/0/+45/-45/0/0/0/0/90/0/0/0/+45/-45]_S$	56%/38%/6%

[a]All ply thickness is 0.184 mm except for the skin of existing datum design, which is 0.25 mm.

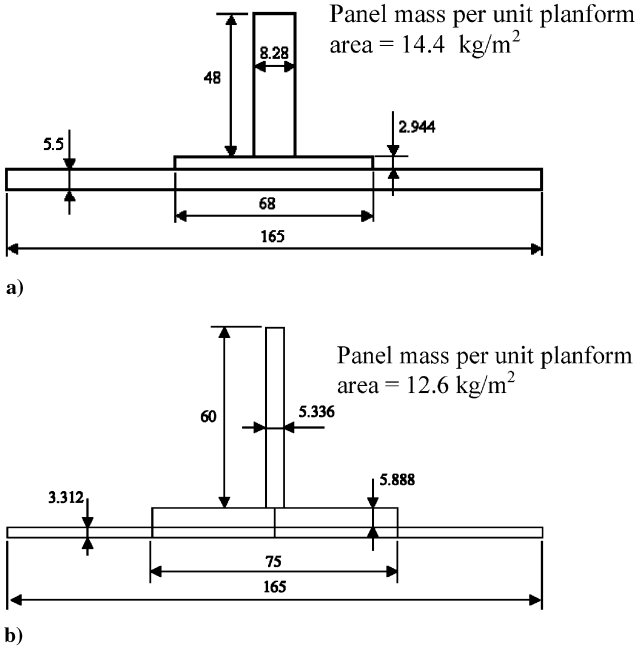

Fig. 12 Cross section of wing cover panel designs. a) Datum design. b) New optimum design. All dimensions in mm.

3600 microstrain. Blade stiffeners have been used in the existing datum design of this aircraft wing and optimization design based on this stiffener shape was used to keep the manufacture process unchanged. Other stiffener shapes have the potential to provide more structural efficiency, but have not been considered here.

Table 5 and Fig. 12b show the new optimum design obtained from the bilevel strategy. Design constraints were applied to the optimization, that is, lower bounds of 68 mm were applied to the stiffener flange and the stiffener spacing was constrained to be 165 mm. It is shown that the strategy reduces the weight of the existing datum design by 13%. In addition, the optimum design was achieved with little computational effort.

V. Concluding Remarks

Experimental testing, and linear and nonlinear FEA were performed on two blade-stiffened panels, which were designed using VICONOPT with initial buckling in the stiffener and skin, respectively. The 3-blade panel, with initial buckling in the stiffener, was less sensitive to imperfection than the 2-blade panel, which had initial buckling in the skin. Both panels buckled in the high load and high strain range, and had little postbuckling capacity, about 7 and 13% above the initial buckling load for the 3-blade and 2-blade panel, respectively. VICONOPT and FEA predictions were in good agreement with experimental data for both panels. Hence the VICONOPT and FE models were validated by the experimental testing.

A bilevel optimization strategy for fast design of composite stiffened panels, using VICONOPT and embracing practical composite design rules, has been presented and performed on the design of a *Z* stiffened panel. The design was analyzed using linear and nonlinear FEA within ABAQUS. Detailed modeling of the root radius of the *Z* stiffener was required otherwise the VICONOPT prediction is about 13% below the experimentally observed initial buckling load/strain. The bilevel optimization described did not account for this radius, and therefore did not find an accurate optimum design. Hence the efficiency of the *Z* stiffened panel, in terms of initial buckling, is lower than that of the blade-stiffened panels; see Table 6, whereas its efficiency in terms of post-buckled failure compares favorably with the blade-stiffened panels. However, it should be noted that all three panels are relatively short and narrow and not therefore representative of aerospace applications such as wing cover panels. It is expected that the efficiency of the *Z* stiffened panel, with its increased overall bending rigidity, would be more favorable than blade-stiffened panels for such applications.

Table 6 Normalized values of structural efficiency (=load/panel weight) for the three panels

Panel	Initial buckling[a]	Failure[a]
3-blade	1.00	1.06
2-blade	1.08	1.23
Z	0.98	1.26

[a]The values of loads are those obtained from the experimental test.

The strategy has also been applied to design a typical wing cover panel with blade stiffener shapes. The strategy showed weight savings of 13% compared with an existing datum design with little computational effort. This has demonstrated that the strategy appears efficient, reliable and extendable into the long panel range. A further advantage is that the laminate design step could easily incorporate manufacturing constraints such as allowing for continuity of plies over rib bays.

Appendix

Equations used to calculate the equivalent orthotropic material properties [15,16] from the laminate [*D*] matrix

$$E_{xx} = \frac{12}{t^3 d_{11}}, \qquad E_{yy} = \frac{12}{t^3 d_{22}}, \qquad G_{xy} = \frac{12}{t^3 d_{66}}, \qquad \nu_{xy} = -\frac{d_{21}}{d_{11}}$$

where

$$d_{11} = \frac{D_{22}D_{66} - D_{26}^2}{|D|}, \qquad d_{22} = \frac{D_{11}D_{66} - D_{16}^2}{|D|}$$

$$d_{12} = \frac{D_{16}D_{26} - D_{12}D_{66}}{|D|}, \qquad d_{66} = \frac{D_{11}D_{22} - D_{12}^2}{|D|}$$

$$d_{16} = \frac{D_{12}D_{26} - D_{22}D_{16}}{|D|}$$

$$d_{26} = \frac{D_{12}D_{16} - D_{11}D_{26}}{|D|}$$

$$\text{with } |D| = (D_{11}D_{22} - D_{12}^2)D_{66} + 2D_{12}D_{26}D_{16} - D_{11}D_{26}^2 - D_{22}D_{16}^2$$

Acknowledgements

The authors would like to thank Martin Gaitonde, Nihong Yang, and Phillip Brown (Airbus U.K. Ltd.) for their valuable assistance. Thanks are also extended to Anthony Elley of the University of Bath for his assistance with the experimental work. This project is sponsored by Airbus U.K. Ltd. and the Department of Mechanical Engineering, University of Bath. VICONOPT is used with the permission of Cardiff University.

References

[1] Venkataraman, S., and Haftka, R. T., "Optimization of Composite Panels: A Review," *Proceedings of the 14th Annual Technical Conference of the American Society of Composites*, Technomic Publishing Co., Lancaster, PA, 17064, 1999, pp. 479–488.

[2] Kollár, L., P., "Buckling of Unidirectionally Loaded Composite Plates with One Free and One Rotationally Restrained Unloaded Edge," *Journal of Structural Engineering*, Vol. 128, No. 9, 2002, pp. 1202–1211.

[3] Kassapoglou, C., "Simultaneous Cost and Weight Minimization of Composite-Stiffened Panels Under Compression and Shear," *Composites, Part A: Applied Science and Manufacturing*, Vol. 28, No. 5, 1997, pp. 419–435.

[4] Butler, R., and Williams, F. W., "Optimum Design Using VICONOPT: A Buckling and Strength Constraint Program for Prismatic Assemblies of Anisotropic Plates," *Computers and Structures*, Vol. 43, No. 4, 1992, pp. 699–708.

[5] Williams, F. W., Anderson, M. S., Kennedy, D., Butler, R., and Aston, G., "User Manual for VICONOPT: An Exact Analysis and Optimum Design Program Covering the Buckling and Vibration of Prismatic Assemblies of Flat In-Plane Loaded, Anisotropic Plates, with Approximations for Discrete Supports, and Transverse Stiffeners," NASA-CR-181966, 1990.

[6] Lillico, M., Butler, R., Hunt, G. W., Watson, A., Kennedy, D., and Williams, F. W., "Analysis and Testing of a Postbuckled Stiffened Panel," *AIAA Journal*, Vol. 40, No. 5, 2002, pp. 996–1000.

[7] Nagendra, S., Jestin, D., Gürdal, Z., Haftka, R. T., and Watson, L. T., "Improved Genetic Algorithm for the Design of Stiffened Composite Panels," *Computers and Structures*, Vol. 58, No. 3, 1996, pp. 543–555.

[8] Anderson, M. S., Stroud, W. J., Durling, B. J., and Hennessy, K. W., "PASCO: Structural Panel Analysis and Sizing Code: User's Manual," NASA Technical Memorandum 80801, Nov. 1981.

[9] Bisagni, C., and Lanzi, L., "Post-Buckling Optimization of Composite Stiffened Panels Using Neural Networks," *Composite Structures*, Vol. 58, No. 2, 2002, pp. 237–247.

[10] Nagendra, S., Haftka, R., T., Gürdal, Z., and Starnes, J. H., Jr., "Design of a Blade Stiffened Composite Panels with a Hole," *Composite Structures*, Vol. 18, No. 3, 1991, pp. 195–219.

[11] Niu, M. C. Y., *Composite Airframe Structures: Practical Design Information and Data*, Conmilit Press, Ltd., Hong Kong, 1992, p. 440.

[12] Lillico, M., Butler, R., Hunt, G. W., Watson, A., and Kennedy, D., "Postbuckling of Stiffened Panels Using Strut, Strip, and Finite Element Methods," *AIAA Journal*, Vol. 41, No. 6, 2003, pp. 1172–1179.

[13] Anon., *ABAQUS Theory and User's Manuals*, Version 6.4, ABAQUS, Inc., Pawtucket, RI, 2003.

[14] Kennedy, D., Ioannidis, G., and Featherston, C. A., "Discrete Optimum Design of Composite Plates Including Longitudinal Voids," *Proceedings of the 6th World Congress on Computational Mechanics* [CD-ROM], Tsinghua University Press, Beijing, 2004.

[15] Tsai, S. W., and Hahn, H. T., *Introduction to Composite Materials*, TECHNOMIC Publishing Co., Inc., 265 Post Road West, Westport, CT 06880, 1980.

[16] Weaver, P. M., "Design Composite Structures: Lay-Up Selection," *Proceedings of Institution of Mechanical Engineers Part G: Aerospace Engineering*, Vol. 216, No. 2, 2002, pp. 105–116.

A. Palazotto
Associate Editor